Available online at www.sciencedirect.com

ScienceDirect

Procedia CIRP 49 (2016) 222 – 226

www.elsevier.com/locate/procedia

The Second CIRP Conference on Biomanufacturing

Fiber laser microcutting of AISI 316L stainless steel tubes- influence of pulse energy and spot overlap on back wall dross.

García-López Erika, Medrano-Tellez Alexis, Ibarra-Medina Juansethi, Siller Héctor R., Elías-Zúñiga Alex, Rodríguez Ciro A.*

Escuela de Ingeniería y Ciencias- Centro de Innovación en Diseño y Tecnología, Tecnológico de Monterrey-Campus Monterrey, Av.Eugenio Garza Sada 2501 Sur, CP 64849 Monterrey, Nuevo León, Mexico

* Corresponding author. Tel.:+52 8183582000 ext. 5105 *E-mail address:* ciro.rodriguez@itesm.mx

Abstract

The design of coronary stents imposes high demands in terms of dimensional tolerance and surface finish. These devices are manufactured by laser microcutting of miniature tubes in materials such as stainless steel, cobalt chromium alloys and Nitinol. The work presented here is focused on fiber laser microcutting for coronary struts in AISI 316L stainless steel. This work studies the influence of gases such compressed air and argon passing through the tube in order to drag molten material while laser microcutting is performed. The experimental work studies the influence of beam spot overlap and pulse energy on back wall dross and average surface roughness, using response surface methodology. The results indicate that the introduction of compressed air or argon gas is a relevant method to reduce the amount of dross adhered in the back wall of the miniature tube.

Keywords: back wall dross; fiber laser microcutting; pulse energy; spot overlap

1. Introduction

Coronary stents are cylindrical metal scaffolding that are inserted inside a diseased coronary artery to restore adequate blood flow [1]. This affection is treated with the percutaneous transluminal coronary angioplasty (PTCA) with 500, 000 cases per year in the United States alone [2].

Laser cutting is the most often process to manufacture coronary stents. Comparing laser sources to produce medical devices, fiber lasers have many advantages in contrast with Nd-YAG lasers. For example laser life of Nd-YAG technologies is about ten times less than fiber lasers and at the same time operating costs are increased in Nd-YAG technologies [3].

Although several studies have been conducted to study laser cutting parameters (pulse frequency, pulse width, peak power, cutting speed, gas pressure, gas type and stand-off distance) on surface roughness and dross height, documented research on back wall dross is limited.

Kleine et al. established cutting speed and laser pulse length as the significant terms in order to improve surface roughness in fiber laser cutting of stainless steel material after running an ANOVA analysis [4].

Similarly, Muhammad et al. explained that increasing the pulse width, the material/ beam interaction time is highest, which increases the kerf width and surface roughness for fiber laser cutting of AISI 316L stainless steel material [5].

Adelman et al. conducted a study using a multi-mode fiber laser and it was concluded that gas pressure and focus position are significate parameters for burr height [6].

Pfeifer et al. reported the influence of stand-off distance on speed rate of the gas and its effects on cutting performance and geometry using a pulsed Nd-YAG laser [7].

doi:10.1016/j.procir.2015.11.020

Teixidor et al. characterized geometrically dross height based on energy balances in fiber laser cutting [8].
Some of the issues considered in high precision manufacturing include slag, burrs, surface roughness, heat affected zones and dross adhesion, these quality problems are solved adjusting cutting parameters.
In laser processing, various processing parameters can be combined into fewer more abstract process parameters. Pulse overlapping factor, O_f, is associated to the periodic striation on the cut edge produced in pulsed mode and it is given by equation (1), where v is the cutting speed, f is the pulse frequency, and d is the spot diameter [9].

$$O_f = 100\left(1 - \frac{v}{fd}\right) \quad (1)$$

According to Thawari et al. these patterns affect cut quality attributes like surface roughness, kerf width, and surface morphology. As pulse overlap factor decreases, the kerf width tends to decrease and the surface roughness tends to increase [9].
Abdel Ghany explained that the percentage for low striation cuts is around 75 %< spot overlap<80 % and for typical cuts 50 %< spot overlap <70 % for 1.2 mm austenitic stainless steel sheets using pulsed Nd:YAG laser [10].
On the other hand, pulse energy of the laser is related with peak power and pulse frequency by the expression [9]:

$$Pulse\ energy = Peak\ power * Pulse\ width \quad (2)$$

Pfeifer R., et al. observed that surface roughness decreases, increasing laser power and as consequence the pulse energy in laser cuts using a pulsed Nd-YAG laser to cut 1 mm thick NiTi shape memory alloys [7].
The objective of this research is to measure dross in the opposite side of the cut using three treatments; passing compressed air, argon gas and a control test to evaluate differences among dross adherence. In this paper the effect of pulse overlap and pulse energy is presented for AISI 316L stainless steel tubes.

2. Back wall dross

Back wall damage is a challenge for laser cutting of coronary stents. Molten material is deposited on the opposite of wall of tube affecting surface finish.
Muhammad et al. analysed qualitatively the fiber laser cutting of stainless steel 316L tube and the effect of introducing water flow in tubes on back wall dross affectations [5].
Also, some patents explain some methods in order to drag molten material. Tessier et al. presented a coolant system that is pumped through the inner portion of the workpiece before and during laser cutting [11].The dross formed into the coolant, solidifies and is flushed out of the workpiece along with the coolant.

Baxter et al. described a system to introduce oxygen gas through the workpiece as it being laser cut to oxidize any slag or dross created during the laser cutting process. Oxygen or a mixture of oxygen with other gases cools the slag and the workpiece while at the same time oxidizing the slag before it strikes an exposed surface of the tubular member [12]. Bialas et al. presented a method to use a sacrificial material masking in at least a portion of the inner surface of the tubular member while laser cut is performed [13]. In this study, back wall dross is quantified with images obtained from a stereomicroscope Carl Zeiss Discovery V8. The total area (2190 µm x 1630 µm) was measured in the middle of tube due to this area was the most influenced by trajectory.
Images were analysed using Image J software in order to quantify the back wall area affected by dross, this value was divided by the total area and then multiplied by 100 to obtain a back wall dross percentage. Figure 1 presents the back wall dross measurement in coronary struts.

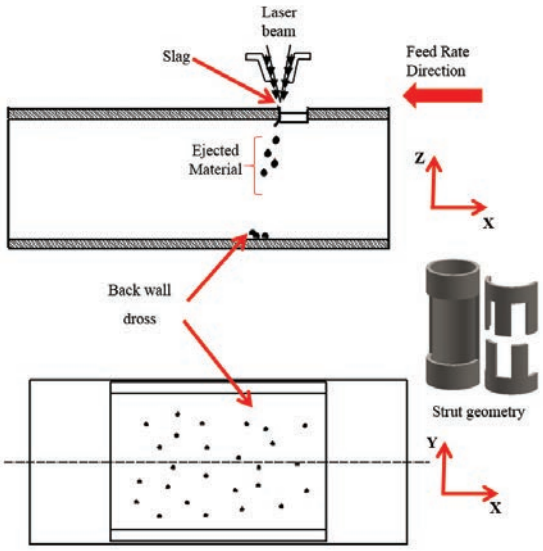

Fig. 1. Back wall dross measurement

3. Materials and methods

A MedPro fiber laser workstation from PRECO Company was used in this work, the features of laser source are presented in Table 1 and experimental setup is illustrated in Figure 2. Laser beam was focused with a focal lens of 50 mm and a 120 mm collimator resulting in a theoretical minimum spot size of 20.8 µm. Experiments were performed in AISI316L stainless steel tubes with outer diameter of 3 mm and 0.22 mm wall thickness. A surface response methodology (SRM) of two factors and 14 runs with three replicates was used to evaluate surface roughness (Ra) and back wall dross percentage. Average surface roughness was measured on cut edge using a confocal microscope AXIO CSM 700.

Spot overlap was calibrated for different cutting speeds and pulse frequencies. Also, pulse energy was established according to peak power and pulse width parameters. Nitrogen gas was used as assisted gas and it was fixed at 150 Psi of pressure during experiments.

Table 1. Laser source features

Characteristic	Conditions	Unit
Nozzle diameter	0.5	mm
Stand-off distance	0.25	mm
Operation mode	CW (modulated)	
Wavelength (λ)	1070	nm
Beam parameter product	1	mm mrad
M^{2-}	2.82	
Maximum average power (CW)	250	W
Maximum peak power (Pulsed)	1500	W
Pulse width (Pulsed mode)	0.2-10	ms

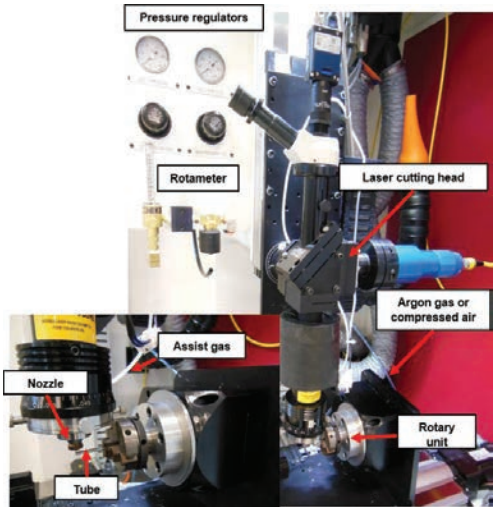

Fig. 2. Experimental setup

Table 2 presents the cutting parameters for surface response methodology. In this work, it was investigated the influence of argon gas and compressed air as external gases to test its influence on drag laser melt particles. When laser cut was executed, these external gases were passed through tubes meanwhile strut geometry was completely cut. In addition a control test was done without passing anything through tubes and just using assist gas. Figure 3 presents the treatments used to drag molten material (a) Control treatment and (b) Using argon gas or compressed air.

Table 2. Cutting parameters for surface response methodology

Cutting Parameter	Level
Spot overlap (%)	30.8-93
Pulse energy (mJ)	32.1-34.3
Assist gas (N_2)	150 Psi
Argon gas	30 Psi (23.6 LPM)
Compressed air	30 Psi (23.6 LPM)

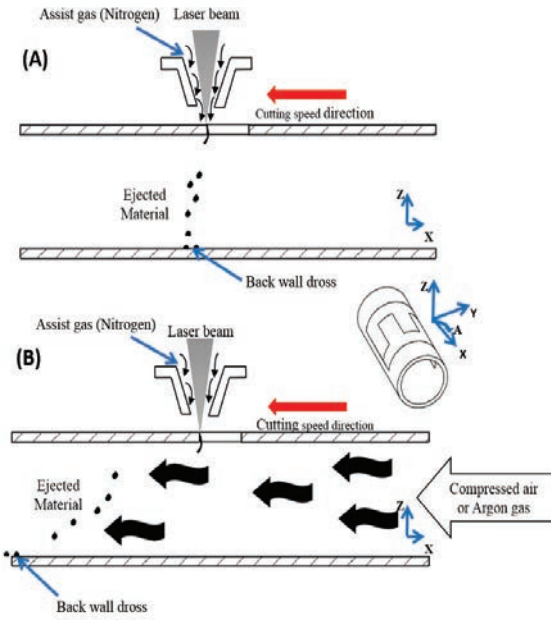

Fig. 3. Treatments to drag molten material (a) Control treatment, (b) Compressed or argon treatment.

4. Results and discussions

Muhammad et al. presented a qualitative study of dross deposition after passing continues water through tube in order to carry away hot particles after they are ejected [5]. Their results showed that wet cutting seems to be effective in preventing the back wall damage.

In this study, the results indicate that the control test (a) reveal a back wall dross percentage between 0.8% and 6%. Meanwhile, the use of compressed air (b) reduces back wall dross range between 2 % and 0.8% and the use of argon gas (c) passed through tubes reduces back wall dross range between 1.4 % and 0.5 % using the same cutting parameters. Figure 4 presents the surface response plots and Table 3 presents the ANOVA results and the coefficient of determination for back wall dross response.

On the other hand, for average surface roughness response, minimum values between 0.5 µm and 0.8 µm are presented for a spot overlap between 80 % and 93 % and a pulse energy range between 32 mJ and 34 mJ. Figure 5 presents the surface response plots and Table 4 presents the ANOVA results for average surface roughness. This tendency is in agreement with Thawari et al. who demonstrated that spot overlap plays a crucial role in pulsed Nd:YAG laser cutting of nickel- base superalloys [9]. Their results reveal that kerf width decrease with decrease in spot overlap while the surface roughness increases. Also, Thawari et al. demonstrated a range between 50 % and 80% of spot overlap and 2.88 J of pulse energy to minimize surface roughness (4 µm and 6 µm). Although values of average surface roughness are different, this is presumably due to the different working parameters and materials experimented.

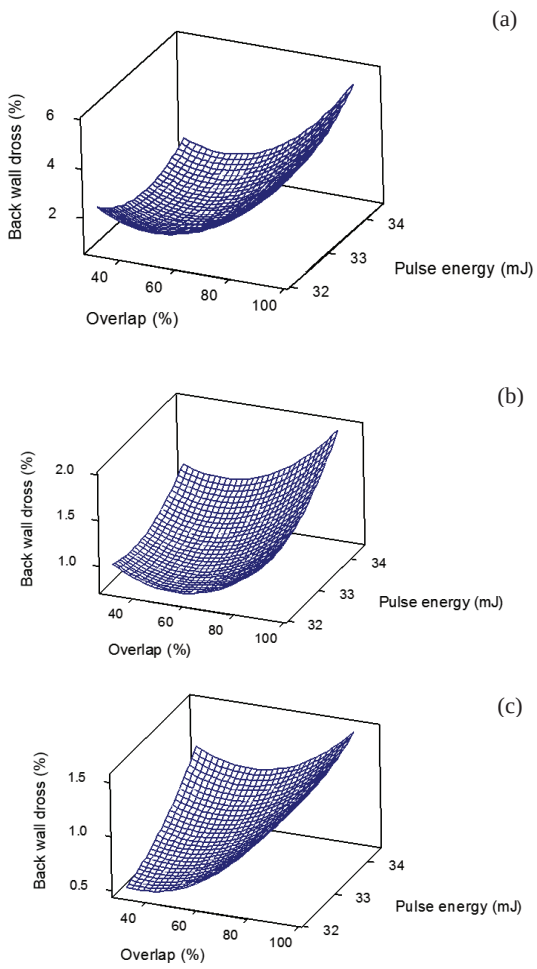

Fig. 4. Back wall dross: (a) control treatment, (b) compressed air, (c) argon gas

Table 3. Anova results for back wall dross percentage.

Treatment	Control treatment			Compressed air		Argon gas	
Response	Dross			Dross		Dross	
R^2-adj	80.4			88.4		82.9	
Source	GL	SS	P	SS	P	SS	P
Blocks	1	0.00	0.99	0.07	0.02	0.07	0.14
Regression	5	13.6	0.01	0.71	0.00	0.74	0.02
Linear	2	10.5	0.01	0.46	0.00	0.56	0.01
Overlap	1	10.4	0.00	0.21	0.00	0.42	0.00
P. energy	1	0.07	0.70	0.25	0.00	0.14	0.05
Quadratic	2	5.53	0.02	0.24	0.00	0.16	0.09
Overlap* Overlap	1	4.15	0.01	0.18	0.00	0.14	0.04
P.energy *P. energy	1	1.37	0.11	0.06	0.03	0.02	0.38
Interaction	1	0.08	0.67	0.01	0.34	0.02	0.38
Overlap* P. energy	1	0.83	0.67	0.01	0.34	0.02	0.38
Res. error	7	2.01		0.05		0.09	
Lack of fit	3	1.97	0.17	0.01	0.85	0.07	0.45
Pure error	4	0.03		0.04		0.02	
Total	13	18.9		0.84		0.97	

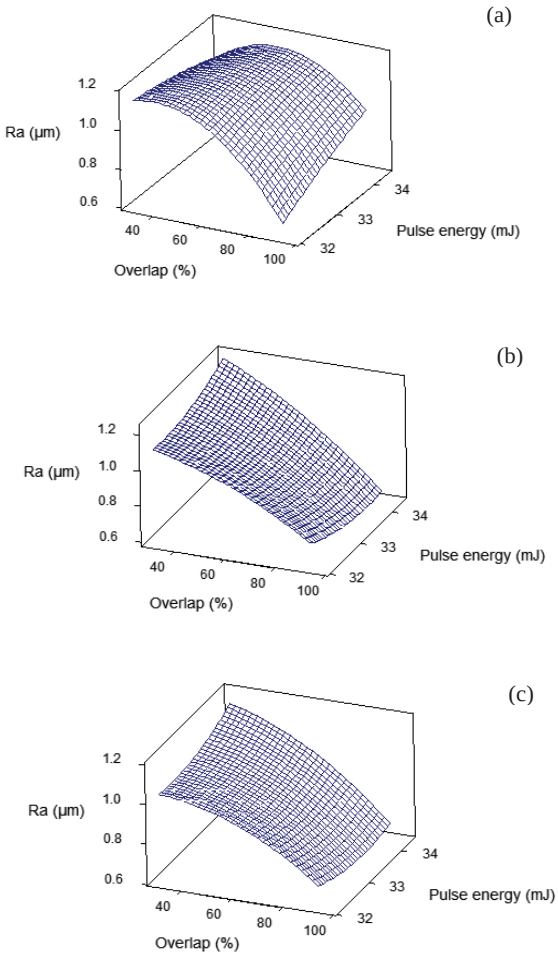

Fig. 5. Average surface roughness (a) control treatment, (b) compressed air, (c) argon gas

Table 4. Anova results for average surface roughness.

Treatment	Control treatment			Compressed air		Argon gas	
Response			Ra		Ra		Ra
R^2-sq			80.2		98.9		95.5
Source	GL	SS	P	SS	P	SS	P
Blocks	1	0.01	0.22	0.00	0.01	0.00	0.12
Regression	5	0.15	0.01	0.26	0.00	0.18	0.00
Linear	2	0.09	0.00	0.25	0.00	0.16	0.00
Overlap	1	0.09	0.00	0.25	0.00	0.16	0.00
P. energy	1	0.00	0.33	0.00	0.47	0.00	0.24
Quadratic	2	0.05	0.02	0.01	0.00	0.01	0.01
Overlap* Overlap	1	0.05	0.01	0.01	0.00	0.01	0.01
P.energy *P. energy	1	0.00	0.69	0.00	0.01	0.00	0.06
Interaction	1	0.01	0.17	0.00	0.01	0.00	0.18
Overlap* P. energy	1	0.01	0.17	0.00	0.01	0.00	0.18
Res. error	7	0.02		0.00		0.00	
Lack of fit	3	0.01	0.34	0.00	0.26	0.00	0.65
Pure error	4	0.01		0.00		0.00	
Total	13	0.18		0.26		0.19	

Experimental models from statistical analysis were obtained according to significant cutting parameters. These models are presented in Table 5 and are valid for cutting parameter levels established in Table 2.

Table 6 presents a qualitative study for back wall dross and average surface roughness. It is observed the lowest amount of dross adhered in the opposite side of the cut using compressed air and argon gas (see conditions *b* and *c* in Table 6) compared with control treatment (see condition *a* in Table 6).

Table 5. Response surface models

Control treatment	
$Ra = 1.12 - 0.149 \times Overlap - 0.170 \times Overlap^2$	(3)
$Back\ wall\ dross = 1.16 + 1.41 \times Overlap + 1.561 \times Overlap^2$	(4)
Compressed air	
$Ra = 0.926 - 0.24 \times Overlap - 0.052 \times Overlap^2 + 0.040 \times Pulse\ energy^2 - 0.05 \times Overlap \times Pulse\ energy$	(5)
$Back\ wall\ dross = 0.880 + 0.23 \times Overlap + 0.25 \times Pulse\ energy + 0.328 \times Overlap^2 + 0.181 \times Pulse\ energy^2$	(6)
Argon gas	
$Ra = 0.913 - 0.202 \times Overlap - 0.069 \times Overlap^2$	(7)
$Back\ wall\ dross = 0.762 + 0.322 \times Overlap + 0.184 \times Pulse\ energy + 0.282 \times Overlap^2$	(8)

Table 6. Cutting qualities for back wall dross and average surface roughness

Control treatment
Spot overlap 61.9%, Pulse energy 33.2 mJ
a) Ra < 1 µm D<3 %

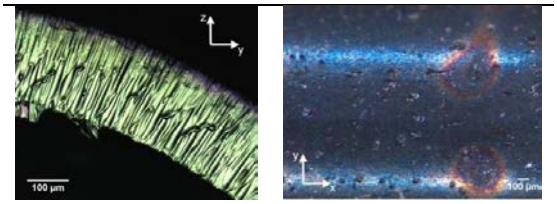

Compressed air
Spot overlap 61.9%, Pulse energy 33.2 mJ
b) Ra<1µm D<1%

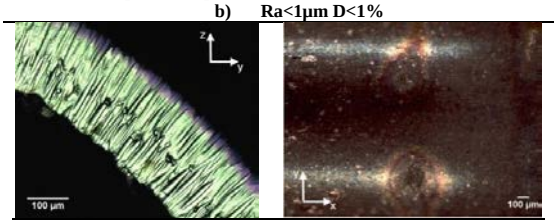

Argon gas
Spot overlap 61.9%, Pulse energy 33.2 mJ
c) Ra<1µm D<1%

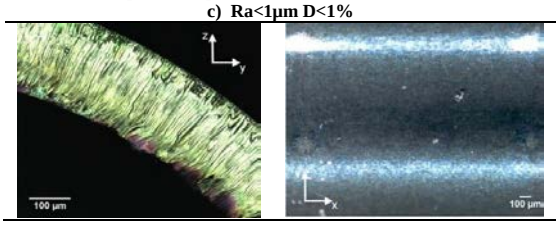

5. Conclusions

This study was focused on assessing the influence of process parameters on average surface roughness (R_a) and back wall dross during fiber laser microcutting of miniature stainless steel tubes, with potential applications in medical implants such as coronary stents.

The response surface plots indicate that the highest level of spot overlap (60% to 93%) reduces average surface roughness. Also, passing compressed air or argon gas reduces back wall dross. The control treatment shows 6% of back wall dross, while minimum values of 1.5% to 2% were obtained using compressed air and argon gas. The study concludes that passing an external gas through the miniature tubes, as a method for dragging molten particles produced by laser microcutting, is an effective approach to reduce back wall dross.

Acknowledgements

This research was possible with support from the grant FOMIX NL-2010-C30-145045 and from Tecnológico de Monterrey, through the research group in Advanced Manufacturing.

References

[1] Whittaker, D., & Fillinger, M. (2006). The engineering of endovascular stent technology: a review. *Vasc Endovascular Surg.*, *40*(2), 85-94
[2] Eberhart, R., Su, S., Nguyen, K., Zilberman, M., Tang, L., Nelson, K., & Frenkel, P. (2003). Bioresorbable polymeric stents: current status and future promise. *J Biomater Sci Polym Ed.*, *14*(4), 299-312.
[3] IPGphotonics. (2015) http://www.ipgphotonics.com/apps_materials_multi_advantages_htm.
[4] Kleine, K., Whitney, B., & Watkins, K. (2002). Use of Fiber Lasers for Micro Cutting Applications in the Medical Device. *ICALEO*, (pp. 1-10). Scottsdale, USA.
[5] Muhammad, N., Whitehead, D., Boor, A., & Li, L. (2010). Comparison of dry and wet fibre laser profile cutting of thin 316L stainless steel tubes for medical device applications. *Journal of Materials Processing Technology*, *210*(15-19), 2261-2267.
[6] Adelmann, B., & Hellmann, R. (2011). Fast Laser Cutting Optimization Algorithm. *Physics Procedia*, *12*(A), 591-598.
[7] Pfeifer, R., Herzog, D., Hustedt, M., & Barcikowski, S. (2010). Pulsed Nd:YAG laser cutting of NiTi shape memory alloys—Influence of process parameters. *Journal of Materials Processing Technology*, *210*(14), 1918-1925.
[8] Teixidor, D., Ciurana, J., & Rodríguez, C. (2014). Dross formation and process parameters analysis of fibre laser cutting of stainless steel thin sheets . *Int J Adv Manuf Technol*, 1611-1621.
[9] Thawari, G., Sarin, S., Sundararajan, G., & Joshi, S. (2005). Influence of process parameters during pulsed Nd:YAG laser cutting of nickel-base superalloys. *Journal of Materials Processing Technology*, *170*(1-2), 229-239.
[10] Ghany, K., & Newishy. (2005). Cutting of 1.2mm thick austenitic stainless steel sheet using pulsed and CW Nd:YAG laser. *Journal of Materials Processing Technology*, *168*, 438-447.
[11] Tessier, J., & Brown, W. (1991). *United States Patent No. US5073694.*
[12] Baxter, W., & Mackiewicz, D. (2014). *United States Patent No. 0312005 A1.*
[13] Bialas, M., Simpson, J., & Barbier, R. (2011). *United States Patent No. 7932479 B2.*